

First-Principles Modeling of Dopants in C₂₉ and C₂₉H₂₄ Nanodiamonds

A. S. Barnard,[†] S. P. Russo,^{*,‡} and I. K. Snook[‡]

Center for Nanoscale Materials, Argonne National Laboratory, 9700 South Cass Avenue, Argonne, Illinois 60439, and Applied Physics, School of Applied Sciences, RMIT University, GPO Box 2476V, Melbourne 3001, Australia

Received: March 23, 2005; In Final Form: April 26, 2005

Presented here is our continuing first-principles density functional theory study of the structural stability of a select group of dopants in diamond nanocrystals. On the basis of the work of others concerning dopants in diamond and endohedral atoms in fullerenes, the dopants selected for use here are oxygen, aluminum, silicon, phosphorus, and sulfur. These atoms were included substitutionally in the center of a 29-carbon-atom nanodiamond crystal, and each structure was relaxed using the Vienna Ab Initio Simulation Package. We describe the bonding and structure of the relaxed doped nanocrystals via examination of the electron charge density and point group symmetry. In combination with our previously reported results, it is anticipated that these results will assist in providing a better understanding of the mechanical stability of doped nanodiamonds for use in diamond nanodevices.

1. Introduction

As the doping of diamond has led to the invention many electronic and optoelectronic devices,¹ the doping of nanocrystalline diamond^{2,3} and films generated using chemical vapor deposition (CVD)⁴ is currently receiving considerable attention. For electronic uses, one of the main objectives in the doping of nanocrystalline diamond is the production of stable p-type and n-type semiconductor materials, while for quantum computing the main objective is to find stable dopants with suitable spin states.⁵ However, before the electronic or spin properties of impurities in nanodiamond may be examined, it is first important to establish which dopant species may be expected to be stable within the nanodiamond lattice. This is the topic of the present study, beginning with a synopsis of the doping of bulk diamond.

The doping of bulk diamond with a wide variety of elements has been the topic of numerous theoretical and experimental studies over the past few decades. Suitable dopants include a variety of elements including metals and semiconductors.⁶ For example, doping single-crystal⁷ and CVD⁸ diamond with silicon produces a Si center, which has been found to increase photoluminescence upon annealing in the temperature range of maximum hole mobility.⁹ Doping of CVD diamond with metals such as palladium has also been achieved. In this case, the Pd clusters in the Pd-doped films promote deposition from a gas-phase precursor, facilitating subsequent selective metal deposition on the doped film.¹⁰ The most common objective in the doping of diamond is, however, to create p-type or n-type semiconducting materials.

Although boron remains the most successful p-type dopant, potassium, sodium, and aluminum doping of diamond have been achieved by forced diffusion, with results showing shallow acceptor levels in the cases of K and Na and deep acceptor levels in the case of Al.¹¹ Recently, hydrogen-acceptor-level

interactions have been investigated via deuterium diffusion in B-doped diamond.¹²

The search for a suitable n-type dopant of diamond has not been as successful. In theory, possible donors in diamond include lithium (interstitial),^{13,14} sodium (interstitial),^{13,14} nitrogen (substitutional),¹⁵ phosphorus (substitutional), arsenic (substitutional), antimony (substitutional),^{16,17} and sulfur.^{18–20} Phosphorus^{14,21–24} has been found to have a donor level.¹⁹ However, the electron mobility values achieved so far for CVD-grown P-containing diamond layers are still rather low. Limited donor level success has been reported with sulfur, but due to some B contamination found in the S-doped samples, more work is required.²⁵ Lithium has been found to offer only very shallow donor levels.¹¹ Oxygen has also been introduced as an n-type donor²⁶ in diamond. There are indications that conduction due to the presence of the implanted O has been observed; however, the study²⁶ does not definitively prove n-type conductivity. A study has also been conducted on the iodine doping of amorphous carbon.²⁷ No experimental evidence has been found to support the n-type doping of diamond with Na, As, or Sb.

Theoretical studies have also been undertaken investigating various complexes of dopants in bulk diamond^{20,28} and experimental studies regarding the doping of natural diamond by diffusion of boron, lithium, oxygen, hydrogen, and nitrogen into natural transparent type IIa diamond.²⁹

2. Doping of Nanodiamond Crystals

Previous studies on the structural and electronic properties of substitutional dopants within bulk diamond^{30,31} have shown that such impurities affect only the local region surrounding the defect and are (to first approximation) limited to the first nearest neighbors in the lattice. It is therefore feasible to model the effects of dopants in nanodiamonds using a suitably small centro-symmetric cluster. The cuboctahedral dehydrogenated C₂₉ nanodiamond cluster selected for use in this (and previous) studies has been generated with a surface area comprised by 40% {111} (eight triangular faces) and 60% {100} (six square faces). The hydrogenated version, C₂₉H₂₄, has the same structure

* Author to whom correspondence should be addressed. E-mail: salvy.russo@rmit.edu.au.

[†] Argonne National Laboratory.

[‡] RMIT University.

as the C_{29} nanocrystal, with all of the dangling surface bonds terminated with hydrogens.^{2,32,33} The dopant atoms have been inserted substitutionally into the centro-symmetric lattice site of a “cleaved” dehydrogenated structure and into a prerelaxed hydrogenated structure. Therefore, any changes in the hydrogenated crystal structure were known to be due to the inclusion of the dopant, and the length of simulation time was reduced. Although the C_{29} nanodiamond represents a lower boundary of the size of nanodiamonds, through the use of this cluster the dehydrogenated structures will have local order similar to dopants positioned at the surface of nanodiamonds, and the hydrogenated structures have local order similar to dopants positioned at the center of a nanodiamond crystal.

Also, as our current study concerns the structural stability of doped nanodiamonds rather than the structural properties of endofullerenes, once the stability (or instability) of any particular doped nanodiamond has been determined, little attention has been devoted to the effects of the resulting endohedral dopant on the final fullerene cage. Many rigorous investigations have been undertaken on the properties of endohedral atoms in fullerenes (endofullerenes), including studies of the electronic structure and chemical stabilization of the tetravalent C_{28} fullerene with a variety of endohedral complexes.³⁴ These endohedral complexes, denoted as $M@C_{28}$ (M = various elements), include group IV elements³⁵ carbon,^{36–38} silicon,^{36,39} germanium,^{36,39} and tin^{36,39} as well as aluminum,³⁹ boron,³⁷ calcium,³⁹ copper,³⁷ chromium,³⁷ fluorine,³⁹ hafnium,⁴⁰ iron,³⁷ magnesium,³⁹ nitrogen,³⁷ oxygen,³⁷ scandium,^{37,39} sulfur,³⁹ titanium,^{37–41} uranium,⁴⁰ vanadium,³⁷ and zirconium.^{38–40} In addition to this, the interesting case of Li_8 inside the cage structure of carbon C_{46} clathrate has also been examined previously using first-principles methods.⁴²

2.1. First-Principles Method. Both the dehydrogenated and hydrogenated doped nanodiamonds have been relaxed using the Vienna Ab Initio Simulation Package (VASP).^{43,44} We used ultrasoft, gradient-corrected, Vanderbilt-type pseudopotentials⁴⁵ as supplied by Kresse and Hafner,⁴⁶ and the valence orbitals are expanded on a plane-wave basis up to a kinetic energy cutoff. The crystal relaxations were performed in the framework of density functional theory (DFT) within the generalized gradient approximation (GGA), with the exchange-correlation functional of Perdew and Wang (PW91).⁴⁷ A detailed description of this technique may be found in ref 48. In this study, both the symmetry and the supercell volume have been relaxed to allow possible expansions or contractions of the entire clusters. All clusters were surrounded by a minimum of 5 Å of vacuum space in all directions, to ensure that there is no interaction with the periodic images in neighboring cells. We have previously performed a number of tests and determined that this amount of vacuum space is sufficient for this purpose.³² In the case of the doped structures, each dopant has been included substitutionally at the centro-symmetric lattice site. We have found previously that the undoped, B-doped, and N-doped dehydrogenated nanocrystals of this type are unstable and relax to form endofullerene complexes but that the hydrogenated counterparts retain the diamond structure upon relaxation.²

We have successfully applied this technique to the relaxation of dehydrogenated,^{32,33} hydrogenated,⁴⁹ and doped² (nonperiodic) nanodiamond structures in the past (with results giving excellent agreement with experiment), offering validity to our approach. It is important to point out that even the sizes of the clusters used here can be prohibitive for higher levels of theory. Few comparative studies have been undertaken using cluster models with more sophisticated quantum-chemical techniques.

A few worth mentioning are the studies of Jones and Oberg²¹ (who applied local-density approximation (LDA) and Gaussian basis functions to the study of P in a 71-atom hydrogenated diamond cluster), Wu and Radovic⁵⁰ (who used Hartree–Fock and B3LYP with Gaussian basis functions to study B in graphitic carbon clusters), and the studies of Brown et al.⁵¹ and Huang et al.⁵² (who used ab initio methods to investigate hydrogen abstraction and the growth of diamond clusters, respectively).

3. Al, Si, and P Doping

In light of our results for undoped, B-doped, and N-doped nanodiamonds,² the third-row analogues Al, Si, and P have been considered. In our previous study, we determined that the effects on crystalline stability of the second-row one-electron acceptor B and donor N were similar to an undoped structure. The dehydrogenated structures all relaxed to form endofullerenes $M@C_{28}$ (M = B, C, and N), while the hydrogenated counterparts all retained the diamond structure following the relaxation.²

In the present study, the aluminum dopant was bound to the nearest neighbors in the initial diamond structure; however, results of the relaxation (characterized via the final charge density) revealed that the surrounding nanodiamond shell became a fullerene, producing the $Al@C_{28}$ structure. While the final endoatom–cage distance was within the Al–C bond length, the aluminum atom was not bound to the fullerene cage, although it did remain centered. This suggests a cage–atom interaction via charge transfer, resulting in weak ionic bonding,³⁶ which is further supported by recent findings concerning Al in bulk diamond³⁰ where the bonding was determined to be more ionic than covalent. However, the charge density maps of the hydrogenated nanodiamonds doped with aluminum revealed that while the structure relaxed the central dopant appears only weakly bound (if at all) to the surrounding carbon atoms, and a reasonable degree of relaxation was evident in the final structure, shown in Figure 1.

In the case of the Si-doped dehydrogenated nanocrystal, the silicon atom became an endohedral complex of the final structure. Inspection of the charge density maps showed that residual charge density in the center of the final $Si@C_{28}$ structure appears localized in the region of the initial Si–C bonds. It was again anticipated that the silicon-doped hydrogenated structures would relax in a similar fashion as the undoped nanodiamond, retaining the stable nanodiamond structure. This was found to be the case, although a certain amount of relaxation of the structure occurred (see Figure 2).

The phosphorus dopant was strongly bound to the surrounding carbon atoms in the initial structure, but appeared as an endohedral complex of the final structure ($P@C_{28}$). In addition to this transformation, the endoatom shifted from the center of the cage, which has become distorted by the presence of the unbonded dopant, as indicated in by Figure 3. The phosphorus endoatom shifted sufficiently as to bond with the carbon atoms of the C_{28} fullerene. In the hydrogenated nanodiamond, however, the phosphorus dopant remained in the center of the crystal; the bonds connecting the dopant atom to the surrounding carbons remain intact, and the nanodiamond structure persisted following relaxation. The excess charge due to the extra valence electrons of phosphorus atoms could be seen in the charge density maps as a halo around the central atom.

4. O and S Doping

Also considered in this study are the group VI donors O and S. The oxygen dopant was strongly bound to the surrounding carbon atoms in the initial dehydrogenated structure, but

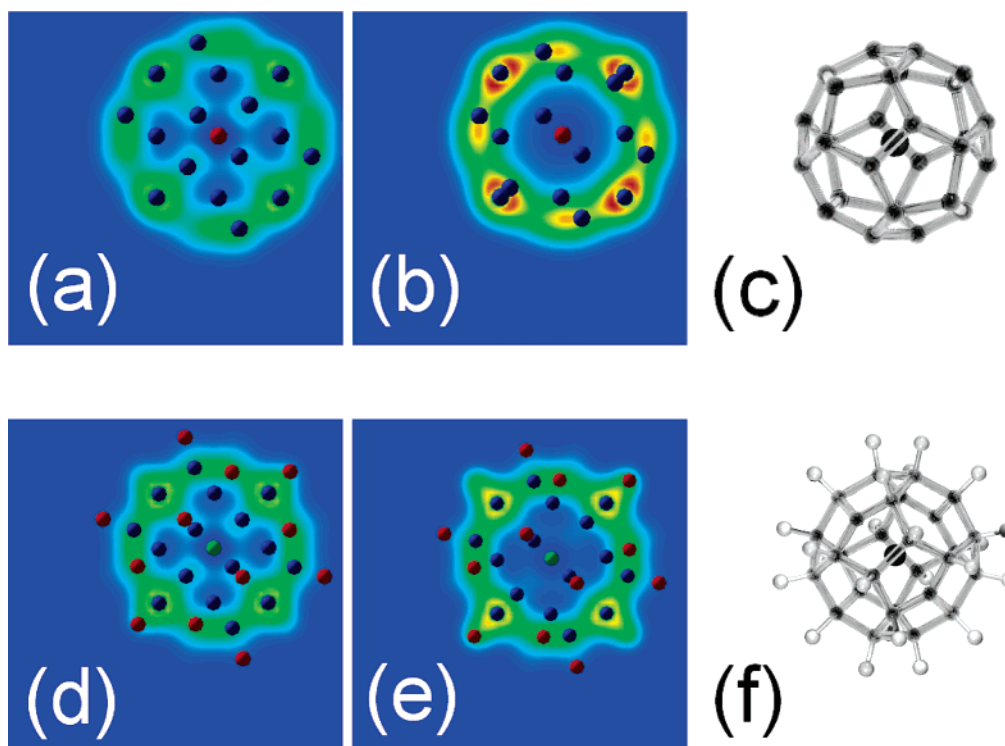


Figure 1. Electron charge density maps through the central (100) plane of the (a) initial and (b) relaxed dehydrogenated Al-doped nanodiamond and the (d) initial and (e) relaxed hydrogenated Al-doped nanodiamond, viewed from the [100] direction. Images showing the relaxed (c) dehydrogenated and (f) hydrogenated structures are also given.

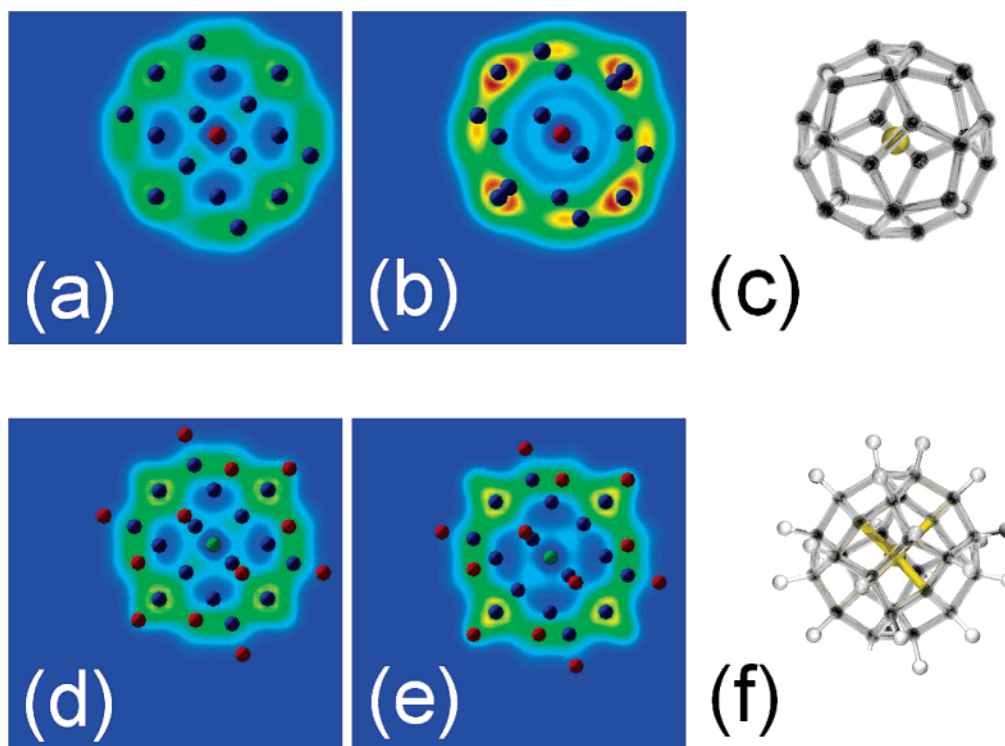


Figure 2. Electron charge density maps through the central (100) plane of the (a) initial and (b) relaxed dehydrogenated Si-doped nanodiamond and the (d) initial and (e) relaxed hydrogenated Si-doped nanodiamond, viewed from the [100] direction. Images showing the relaxed (c) dehydrogenated and (f) hydrogenated structures are also given.

appeared as an endohedral complex of the final structure, $O@C_{28}$. In addition to this transformation, the endoatom shifted from the center of the cage, which became distorted by the presence of the endohedral atom. In a fashion similar to the dehydrogenated O-doped nanodiamond, the oxygen atom becomes an endohedral complex, and the $O@C_{28}H_{24}$ structure resulted.

The sulfur dopant while bound to the surrounding carbon atoms in the initial dehydrogenated structure appeared as an endohedral complex of the final structure, $S@C_{28}$. In addition to this transformation, the endoatoms shifted from the center of the cage sufficiently as to bond with the carbon atoms of the C_{28} fullerene, which then exhibited pronounced distortion. Similarly, the S-doped hydrogenated crystal not only became a

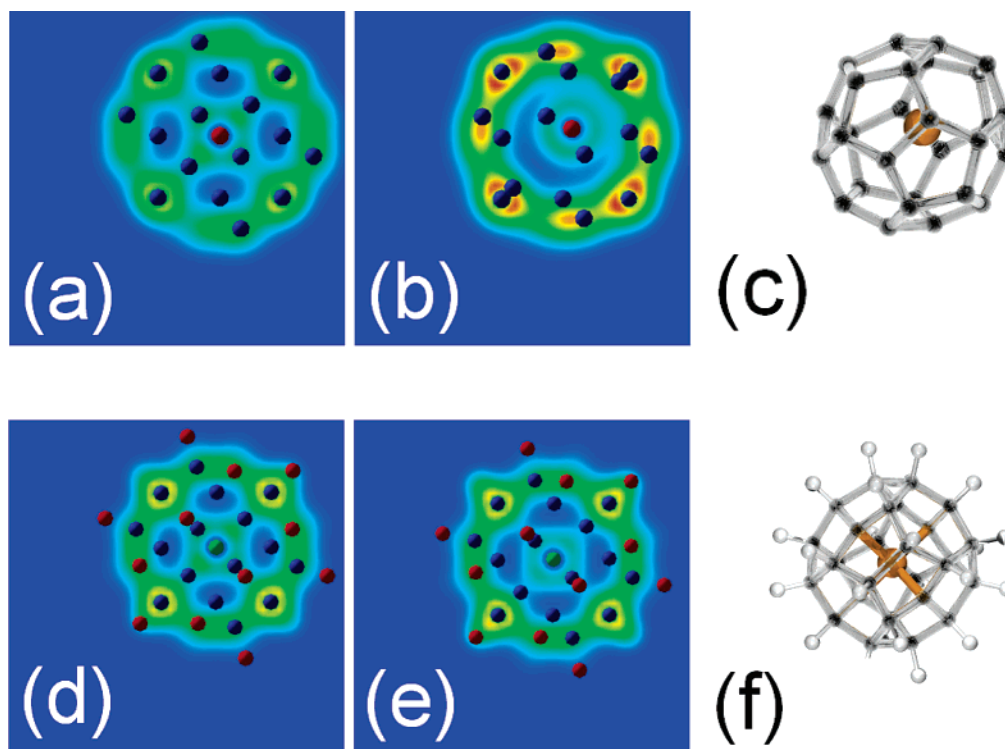


Figure 3. Electron charge density maps through the central (100) plane of the (a) initial and (b) relaxed dehydrogenated P-doped nanodiamond and the (d) initial and (e) relaxed hydrogenated P-doped nanodiamond, viewed from the [100] direction. Images showing the relaxed (c) dehydrogenated and (f) hydrogenated structures are also given.

fullerene, producing the $S@C_{28}H_{24}$ complex, but the sulfur endoatom again shifted from the central position and slightly distorted the hydrogenated carbon cage. This is a unique result among the doped nanodiamond structures.

5. Discussion of Structure and Symmetry

The structural stability of small nanodiamond crystals such as those included in this study may be considered in terms of changes in the symmetry and the carbon framework of the structure, or more precisely, in terms of changes in the point group of the structure. Bulk diamond is characterized by the T_d point group, as are the initial unrelaxed nanodiamonds used here (the “initial” structures). A change in the point group of the cluster upon relaxation or a departure from the T_d point group outside an allowable tolerance therefore represents a type of structural instability.

The point group has been determined for each of the nanodiamond structures using the program SYMMOL,⁵³ based on the work of Pilati and Forni.⁵⁴ The program calculates the quality of fit of an ideal point group to the actual structure, along with the associated uncertainty (error). A large error indicates a poor fit to the ideal point group, although the point group may still be the most appropriate to the structure. It is expected that a certain degree of departure from the ideal bulk diamond point group T_d will be observed due to the fact that the hydrogen atoms have more freedom to adopt nontetrahedral bond angles at the edges and corners of the crystals and that the dissociated dopant atoms may shift from the centrosymmetric position. Therefore, the dopant atoms and hydrogen terminations have been ignored, and the point group calculated only for the carbon framework. The results are contained in Tables 1 and 2 for the unrelaxed and relaxed dehydrogenated and hydrogenated structures, respectively, which contain the point group of best fit and the error.

TABLE 1: Comparison of the Point Groups of the Dehydrogenated, Doped Nanodiamonds before (initial) and after (relaxed) the Relaxation and the Stability of the Dopant within the Nanodiamond, Determined via the Examination of the Respective Charge Density Maps^a

dopant	initial PG	initial error	relaxed PG	relaxed error	stability
lithium	T_d	0.0000	T_d	0.0118	unstable
boron	T_d	0.0000	T_d	0.0036	unstable
carbon (undoped)	T_d	0.0000	T_d	0.0707	unstable
nitrogen	T_d	0.0000	C_{3v}	0.0005	unstable
oxygen	T_d	0.0000	C_{3v}	0.4207	unstable
aluminum	T_d	0.0000	T_d	0.0034	unstable
silicon	T_d	0.0000	T_d	0.0143	unstable
phosphorus	T_d	0.0000	T_d	0.9000	unstable
sulfur	T_d	0.0000	C_{3v}	0.9000	unstable

^a Lithium, boron, nitrogen, and carbon (undoped), while not discussed, have been included for completeness.

Table 1 shows that each dehydrogenated nanocrystal exhibits a deterioration of point group symmetry upon relaxation, with the nanodiamonds doped with nitrogen, oxygen, and sulfur undergoing the largest deteriorations (changing from the T_d to the trigonal C_{3v} point group). The boron dopant (previously found to be the most stable dopant in this cluster²) results in the lowest deterioration of structural symmetry. In the case of the hydrogenated nanodiamonds, sulfur exhibits the largest deterioration (changing from the T_d to the trigonal C_1 point group), while C and N central atoms result in the lowest deteriorations of symmetry. It is interesting to note, however, the change from the T_d to the trigonal C_{3v} point group of the hydrogenated boron-doped nanodiamond caused by the contraction of the C–C bonds lengths of the carbon framework.²

A distortion of this type has been found before by Nishimatsu et al.,²⁸ who performed DFT LDA calculations examining isolated substitutional donor impurities in bulk diamond (phosphorus single-donor, sulfur double-donor, and hydrogen) at

TABLE 2: Comparison of the Point Groups of the Hydrogenated, Doped Nanodiamonds before (initial) and after (relaxed) the Relaxation and the Stability of the Dopant within the Nanodiamond, Determined via the Examination of the Respective Charge Density Maps^a

dopant	initial PG	initial error	relaxed PG	relaxed error	stability
lithium	T_d	0.0000	T_d	0.2451	unstable
boron	T_d	0.0000	C_{3v}	0.0475	stable
carbon (undoped)	T_d	0.0000	T_d	0.0146	stable
nitrogen	T_d	0.0000	T_d	0.0236	stable
oxygen	T_d	0.0000	T_d	0.1102	unstable
aluminum	T_d	0.0000	T_d	0.2523	unstable
silicon	T_d	0.0000	T_d	0.3098	stable
phosphorus	T_d	0.0000	T_d	0.1080	stable
sulfur	T_d	0.0000	C_1	0.0000	unstable

^a Lithium, boron, nitrogen, and carbon (undoped), while not discussed, have been included for completeness.

various sites, along with hydrogen-related complexes (phosphorus–hydrogen and sulfur–hydrogen). In this study, it was reported that the two donor impurities exhibited Jahn–Teller distortions, reducing their symmetries from T_d to C_{3v} ,²⁸ in agreement with the results presented here.

6. Conclusions

We have examined the effects of various dopant species on the bonding and structure of a 29-atom, cuboctahedral nanodiamond. The results of the dehydrogenated, doped nanodiamond relaxations clearly indicate that *none* of these structures are stable. In all cases, the doped nanodiamond underwent a transition to the C₂₈ fullerene structure upon relaxation, irrespective of the dopant. While variations in the final endohedral complexes M@C₂₈ (M = O, Al, Si, P, or S) exist, a detailed discussion of these complexes requires further analysis and is not presented in this study. It has also been illustrated here that not only does doping of this otherwise unstable nanodiamond fail in promoting stability but that group VI two-electron donors produce significant distortion of the surrounding carbon cage. These dopants were also found to be unstable in the hydrogenated clusters.

In conclusion, it has been found that boron, nitrogen, silicon, and phosphorus are the only dopant atoms that are stable in the nanodiamond lattice, as long as the impurities are positioned substitutionally at lattice sites removed from any surfaces or interfaces. Future work is planned along these lines using more sophisticated quantum-chemical techniques.

Acknowledgment. We thank the Victorian Partnership for Advanced Computing and the Australian Partnership for Advanced Computing supercomputer centers for their ongoing assistance over the course of this project. This work was supported in part by the U. S. Department of Energy's Office of Basic Energy Sciences, Division of Materials Science, under Contract No. W-31-109-ENG-38.

References and Notes

- (1) Kalish, R. *Carbon* **1999**, 37, 781.
- (2) Barnard, A. S.; Russo, S. P.; Snook, I. K. *J. Chem. Phys.* **2003**, 117, 10725.
- (3) Albu, T. V.; Anderson, A. B.; Angus, J. C. *J. Electrochem. Soc.* **2002**, 149, E143.
- (4) Kaukonen, M.; Sitch, P.; Jungnickel, G.; Nieminen, R. M.; Pöykkö, S.; Porezag, D.; Frauenhiem, Th. *Phys. Rev. B* **1998**, 57, 9965.
- (5) Park, S.; Srivastava, D.; Cho, K. *J. Nanosci. Nanotechnol.* **2001**, 1, 75.
- (6) Goss, J. P.; Jones, R.; Briddon, P. R. *Phys. Rev. B* **2002**, 65, 035203.

- (7) Sittas, G.; Kanda, H.; Kiflawi, I.; Spear, P. M. *Diamond Relat. Mater.* **1996**, 5, 866.
- (8) Wu, W.-J.; Hon, M.-H. *Surf. Coat. Technol.* **1999**, 111, 134.
- (9) Kiflawi, I.; Sittas, G.; Kanda, H.; Fisher, D. *Diamond Relat. Mater.* **1997**, 6, 146.
- (10) Simakin, A. V.; Loubnin, E. N.; Shafeev, G. A.; Doppelt, P. *Appl. Surf. Sci.* **2001**, 73, 1.
- (11) Popovici, G.; Sung, T.; Prelas, M. A. *J. Chem. Vap. Deposition* **1994**, 3, 115.
- (12) Chevallier, J.; Lusson, A.; Ballutaud, D.; Theys, B.; Jomard, F.; Deneuve, A.; Bernard, M.; Gheeraert, E.; Bustarret, E. *Diamond Relat. Mater.* **2001**, 10, 399.
- (13) Kajihara, S. A.; Antonelli, A.; Bernholc, J.; Car, R. *Phys. Rev. Lett.* **1991**, 66, 2010.
- (14) Kajihara, S. A.; Antonelli, A.; Bernholc, J. *Physica B* **1993**, 185, 144.
- (15) Goss, J. P.; Briddon, P. R.; Jones, R.; Öberg, S. *J. Phys.: Condens. Matter* **2004**, 16, 4567.
- (16) Vavilov, V. S. *Phys.-Usp.* **1994**, 37, 407.
- (17) Vavilov, V. S. *Phys.-Usp.* **1997**, 40, 15.
- (18) Saada, D.; Adler, J.; Kalish, R. *Appl. Phys. Lett.* **2000**, 77, 878.
- (19) Wang, L. G.; Zunger, A. *Phys. Rev. B* **2002**, 66, 161202.
- (20) Miyazaki, T.; Okushi, H. *Diamond Relat. Mater.* **2002**, 11, 323.
- (21) Jones, R.; Öberg, S. *Philos. Mag. Lett.* **1991**, 64, 317.
- (22) Gheeraert, E.; Koizumi, S.; Teraji, T.; Kanda, H.; Nesladek, M. *Phys. Status Solidi A* **1999**, 174, 39.
- (23) Gheeraert, E.; Koizumi, S.; Teraji, T.; Kanda, H.; Nesladek, M. *Diamond Relat. Mater.* **2000**, 2, 948.
- (24) Gheeraert, E.; Casanova, N.; Koizumi, S.; Teraji, T.; Kanda, H. *Diamond Relat. Mater.* **2001**, 20, 444.
- (25) Kalish, R. *Diamond Relat. Mater.* **2001**, 10, 1749.
- (26) Prins, J. F. *Diamond Relat. Mater.* **2000**, 9, 1275.
- (27) Allon-Alaluf, M.; Croitoru, N. *Diamond Relat. Mater.* **1997**, 6, 555.
- (28) Nishimatsu, T.; Katayama-Yoshida, H.; Orita, N. *Jpn. J. Appl. Phys., Part 1* **2002**, 41, 1952.
- (29) Popovici, G.; Wilson, R. G.; Sung, T.; Prelas, M. A.; Khasawinah, S. *J. Appl. Phys.* **1995**, 70, 5103.
- (30) Barnard, A. S.; Russo, S. P.; Snook, I. K. *Philos. Mag. B* **2003**, 83, 1163.
- (31) Goss, J. P.; Briddon, P. R.; Jones, R.; Sque, S. *Diamond Relat. Mater.* **2004**, 13, 684.
- (32) Barnard, A. S.; Russo, S. P.; Snook, I. K. *Philos. Mag. Lett.* **2002**, 83, 39.
- (33) Barnard, A. S.; Russo, S. P.; Snook, I. K. *Diamond Relat. Mater.* **2003**, 12, 1867.
- (34) Jackson, K.; Kaxiras, E.; Pederson, M. R. *J. Phys. Chem.* **1994**, 98, 7805.
- (35) Dunlap, B. I.; Haberlen, O. D.; Roesch, N. *Chem. Phys. Lett.* **1992**, 200, 418.
- (36) Jackson, K.; Kaxiras, E.; Pederson, M. R. *Phys. Rev. Lett.* **1993**, 48, 17556.
- (37) Makurina, Y. N.; Sofronov, A. A.; Gusevb, A. I.; Ivanovsky, A. L. *Chem. Phys. Lett.* **2001**, 270, 293.
- (38) Pederson, M. R.; Laouini, N. *Phys. Rev. B* **1993**, 48, 2733.
- (39) Guo, T.; Smalley, R. E.; Scuseria, G. E. *J. Chem. Phys.* **1999**, 99, 352.
- (40) Guo, T.; Diener, M. D.; Chai, Y.; Alford, M. J.; Haufler, R. E.; McClure, S. M.; Ohno, T.; Weaver, J. H.; Scuseria, G. E.; Smalley, R. E. *Science* **1992**, 257, 1661.
- (41) Haberlen, O. D.; Roesch, N.; Dunlap, B. I. *J. Chem. Phys.* **1992**, 96, 9095.
- (42) Timoshevskii, V.; Connetable, D.; Blase, X. *Appl. Phys. Lett.* **2002**, 80, 1385.
- (43) Kresse, G.; Hafner, J. *Phys. Rev. B* **1993**, 47, RC558.
- (44) Kresse, G.; Hafner, J. *Phys. Rev. B* **1996**, 54, 11169.
- (45) Vanderbilt, D. *Phys. Rev. B* **1990**, 41, 7892.
- (46) Kresse, G.; Hafner, J. *J. Phys.: Condens. Matter.* **1994**, 6, 8245.
- (47) Perdew, J.; Wang, Y. *Phys. Rev. B* **1992**, 45, 13244.
- (48) Furthmüller, J.; Hafner, J.; Kresse, G. *Phys. Rev. B* **1996**, 53, 7334.
- (49) Russo, S. P.; Barnard, A. S.; Snook, I. K. *Surf. Rev. Lett.* **2003**, 10, 233.
- (50) Wu, X. X.; Radovic, L. R. *J. Phys. Chem. A* **2004**, 108, 9180.
- (51) Brown, R. C.; Cramer, C. J.; Roberts, J. T. *J. Phys. Chem. B* **1997**, 101, 9574.
- (52) Huang, R. B.; Xie, S. Y.; Tang, Z. C.; Wang, Y. H.; Huang, W. J.; Chen, H.; Zheng, L. S. *J. Cluster Sci.* **1999**, 10, 383.
- (53) Pilati, T.; Forni, A. *J. Appl. Crystallogr.* **2000**, 33, 417.
- (54) Pilati, T.; Forni, A. *J. Appl. Crystallogr.* **1998**, 31, 503.